**Proceedings of the ASME 2009 International Design Engineering Technical Conferences &
Computers and Information in Engineering Conference
IDETC/CIE 2009
August 30-September 2, 2009, San Diego, USA**

DETC2009-86911

STABILITY OF A SUBMERGED DEFORMABLE BODY

Fangxu Jing*
Aerospace and Mechanical Engineering
University of Southern California
Los Angeles, California 90089
Email: fjing@usc.edu

Eva Kanso
Aerospace and Mechanical Engineering
University of Southern California
Los Angeles, California 90089
Email: kanso@usc.edu

ABSTRACT

We study the stability of passive motion of a fish model. The (articulated body) fish model accounts for the finite dimensions of the fish, its bending stiffness (via the torsional springs at the joints), the unsteadiness of the flow (via the added mass effect) but it does not take into consideration vortex shedding from the trailing edge of the fish. The stability analysis shows that there is a range of parameter values (bending stiffness versus body dimensions) that support stable passive swimming in the direction of the body's length.

1 INTRODUCTION

This paper investigates the stability of a deformable body submerged in perfect fluid. Our primary motivation is to model some aspects of fish swimming. Actual fish seem to alternate between actively controlling their shape and passively responding to the surrounding fluid. A fish actively controlling its shape is modeled in [1] as an articulated body whose shape (i.e., the relative angles between the links forming the articulated body) is controlled or given as a function of time. In this work, we investigate the behavior of a fish when the shape variables are left to passively respond to the surrounding fluid and focus particularly on understanding the stability of translational motions. We consider the same articulated body model as in [1] but do not prescribe the shape deformations. That is, our model consists of a body formed of rigid links, assumed to be identical ellipses for simplicity, connected by hinge joints with torsional springs at the joints to emulate the elasticity of actual fish. The motion of the body-fluid system is described entirely by the body configurations and velocities (see [1, 2]). In other words, our model accounts for the unsteadiness of the flow via the added mass effect but it does not take into consideration vortex shedding from the trailing edge of the fish. The latter could be an important mechanism in passive locomotion and stabilization of the fish and will be addressed in a future work.

The stability of a single submerged ellipse (and ellipsoid) moving at a constant translational velocity along one of its symmetry axis is studied in [2, 3]. The motion along the major axis of symmetry is found to be unstable while that along the minor axis is stable. This seems to suggest that a fish moving with a constant velocity along its major axis of symmetry is unstable. However, the rigid body model does not account for the possibility of passive shape deformations. The question that we investigate is the following: can the presence of passive shape variables change

*Address all correspondence to this author.

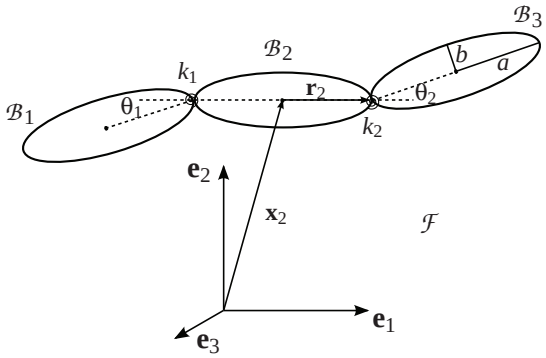

Figure 1. AN ARTICULATED BODY MADE OF THREE IDENTICAL ELLIPSES $\mathcal{B}_i$, $i = 1,2,3$, WITH SEMI-AXES a AND b, CONNECTED BY HINGE JOINTS WITH TORSIONAL SPRINGS k_1 AND k_2, SUBMERGED IN PERFECT FLUID $\mathcal{F}$. THE SHAPE IS PARAMETERIZED BY THE RELATIVE ANGLES θ_1 AND θ_2.

the stability of the problem? Interestingly, the answer is yes. Our analysis predicts a range of parameter values (geometry and torsional stiffness) for which the translational motion of the articulated body along its major axis of symmetry is stable.

It is important to point out that the stability of the submerged deformable body reminds of the flutter of a flag in a breeze. There is a range of critical flow velocities that excite a resonant bending instability causing the flag to flutter or flap stably, see [4, 5]. Obviously the difference between the passive fish and the flag is that the fish itself is moving while the flag is fixed at a given point in a cross-flow. The stability analysis of the flag problem is concerned with the interaction of the shape deformations with the surrounding fluid without accounting for the translational and rotational motions present in the fish problem.

The organization of this paper is as follows. In Section 2, we derive equations governing the motion of the submerged articulated body. The resulting equations admit a number of relative equilibria; the ones of interest correspond to motions of the body at constant velocity along its major axis of symmetry. We investigate the stability of these equilibria in Section 3. We find that, for certain parameter values, these equilibria are stable. The stability results are summarized in Section 4 and Tab. 1.

2 EQUATIONS OF MOTION

2.1 Kinematics

Consider a neutrally buoyant articulated body moving in an infinitely large volume of incompressible, inviscid and irrotational fluid $\mathcal{F}$ at rest at infinity. Let the body be made of N identical rigid ellipses of uniform density ρ (equal to that of the fluid) with semi-axis a and b. The rigid links (or ellipses) are labeled $\mathcal{B}_i$, $i = 1,\ldots,N$, and connected via $N-1$ massless and frictionless hinge joints with torsional spring constants k_i between $\mathcal{B}_i$ and $\mathcal{B}_{i+1}$. An example of three-link body is shown in Fig. 1. It is convenient for studying the locomotion of the system to introduce an inertial frame $\{\mathbf{e}_k\}_{k=1,2,3}$ where $(\mathbf{e}_1,\mathbf{e}_2)$ span the plane of motion and $\mathbf{e}_3$ is perpendicular to the $(\mathbf{e}_1,\mathbf{e}_2)$ plane. Also, one could attach a body-fixed frame $\{\mathbf{b}_k^i\}_{k=1,2,3}$ to the center of mass of each ellipse $\mathcal{B}_i$, where $\mathbf{b}_1^i$ and $\mathbf{b}_2^i$ are parallel to the major and minor semi-axes of the ellipse, respectively, and $\mathbf{b}_3^i \equiv \mathbf{e}_3$. The rigid motion of each ellipse relative to the $\{\mathbf{e}_k\}$ inertial frame can be described by a rotation or proper-orthogonal tensor $\mathbf{Q}_i$ and a translation or position vector $\mathbf{x}_i$ of the mass center. The point transformation from the $\mathcal{B}_i$-fixed frame to the inertial frame can be represented as $\mathbf{x} = \mathbf{Q}_i\mathbf{X} + \mathbf{x}_i$, where $\mathbf{x} = x\,\mathbf{e}_1 + y\,\mathbf{e}_2 + 0\,\mathbf{e}_3$ and $\mathbf{X} = X\,\mathbf{b}_1^i + Y\,\mathbf{b}_2^i + 0\,\mathbf{b}_3^i$. The angular and translational velocities of $\mathcal{B}_i$ expressed in inertial frame are $\boldsymbol{\omega}_i$ and $\dot{\mathbf{x}}_i$, where $\boldsymbol{\omega}_i = \omega_i\mathbf{e}_3$ is the angular velocity vector associated with the skew-symmetric tensor $\dot{\mathbf{Q}}_i\mathbf{Q}_i^T$. The angular and translational velocities expressed in the corresponding body frame are denoted by $\boldsymbol{\Omega}_i$ and $\mathbf{v}_i$, where $\boldsymbol{\Omega}_i = \Omega_i\mathbf{b}_3^i$ is the angular velocity vector associated with the skew-symmetric tensor $\mathbf{Q}_i^T\dot{\mathbf{Q}}_i$ and $\mathbf{v}_i$ is related to $\dot{\mathbf{x}}_i$ by the vector transformation $\dot{\mathbf{x}}_i = \mathbf{Q}_i\mathbf{v}_i$. Let $\mathbf{R}_i = \mathbf{Q}_i^T\mathbf{Q}_{i+1}$ denote the relative rotation of $\mathcal{B}_{i+1}$ with respect to $\mathcal{B}_i$, namely,

$$\mathbf{R}_i = \begin{pmatrix} \cos\theta_i & -\sin\theta_i & 0 \\ \sin\theta_i & \cos\theta_i & 0 \\ 0 & 0 & 1 \end{pmatrix}, \qquad i = 1,\ldots,N-1, \qquad (1)$$

where θ_i is the relative angle between $\mathcal{B}_{i+1}$ and $\mathcal{B}_i$. Let $\mathbf{r}_i$ denote the position vector from the mass center of $\mathcal{B}_i$ to the joint connecting $\mathcal{B}_i$ and $\mathcal{B}_{i+1}$. In body-fixed frame, one has $\mathbf{r}_i = a\mathbf{b}_1^i$. This work specifically considers the cases of two-link and three-link bodies, i.e., $N = 2,3$. Note that one could think of a fully deformable fish model as a limit when the number of joints (or links) goes to infinity ($N \to \infty$).

This undertaking is beyond the scope of the present paper.

2.2 Balances of Momenta

The kinetic energy T of the solid-fluid system can be written as the sum of the energies of the solid links $T_{\mathcal{B}_i}$ and the energy of the fluid $T_{\mathcal{F}}$; namely, $T = \sum_{i=1}^{N} T_{\mathcal{B}_i} + T_{\mathcal{F}}$, where

$$\sum_{i=1}^{N} T_{\mathcal{B}_i} = \frac{1}{2}\sum_i (\mathbf{\Omega}_i \cdot J^{\mathcal{B}} \mathbf{\Omega}_i + \mathbf{v}_i \cdot m^{\mathcal{B}} \mathbf{v}_i)\,. \tag{2}$$

Here, $J^{\mathcal{B}} = m^{\mathcal{B}}(a^2+b^2)/4$ and $m^{\mathcal{B}} = \rho\pi ab$ are the moment of inertia and mass of the identical ellipses, respectively.[1] The kinetic energy of the fluid $T_{\mathcal{F}}$ is given in spatial representation by $T_{\mathcal{F}} = \frac{1}{2}\int_{\mathcal{F}} \rho|\mathbf{u}|^2 \,\mathrm{d}a$, where $\mathbf{u}$ is the spatial velocity field of the fluid and $\mathrm{d}a$ is the standard area element on $\mathbb{R}^2$. For potential flow, the fluid velocity can be written as the gradient of a potential function $\mathbf{u} = \nabla\phi$, where the potential ϕ is the solution to Laplace's equation $\Delta\phi = 0$ subject to the impermeability boundary conditions on the solid boundary, i.e., $\nabla\phi \cdot \mathbf{n}_i = (\mathbf{v}_i + \mathbf{\Omega}_i \times \mathbf{X}_i)\cdot \mathbf{n}_i$ on $\partial\mathcal{B}_i$, and a proper decay at infinity $\nabla\phi = \mathbf{0}$ *at* ∞. Here, $\mathbf{n}_i$ is a unit normal to $\partial\mathcal{B}_i$ and $\mathbf{X}_i$ is the position vector of a point on $\partial\mathcal{B}_i$ relative to the respective mass center. Under these conditions, one can show following a standard procedure (see, for example, [1] and references therein) that $T_{\mathcal{F}}$ can be rewritten as

$$T_{\mathcal{F}} = \frac{1}{2}\sum_i\sum_j (\mathbf{\Omega}_i \cdot \mathbb{J}_{ij}^{\mathcal{F}} \mathbf{\Omega}_j + 2\mathbf{\Omega}_i \mathbb{D}_{ij}^{\mathcal{F}} \mathbf{v}_j + \mathbf{v}_i \cdot \mathbb{M}_{ij}^{\mathcal{F}} \mathbf{v}_j)\,, \tag{3}$$

where $\mathbb{J}_{ij}^{\mathcal{F}}$, $\mathbb{D}_{ij}^{\mathcal{F}}$ and $\mathbb{M}_{ij}^{\mathcal{F}}$ are referred to as the added mass matrices. In general, the components of the added mass matrices are integral functions of the potentials at the solid-fluid boundary and they depend on the geometry and relative angles between the submerged ellipses. In this work, we make the simplifying assumption that the ellipses forming the articulated body are hydro-dynamically decoupled, that is, the added masses for each ellipse can be computed independently of the presence of the remaining ellipses. A direct comparison between the hydro-dynamically decoupled assumption and when $\mathbb{J}_{ij}^{\mathcal{F}}$, $\mathbb{D}_{ij}^{\mathcal{F}}$ and $\mathbb{M}_{ij}^{\mathcal{F}}$ are solved for exactly can be found in [1]. Both approaches give qualitatively similar results. In the hydro-dynamically decoupled case, one has that, for $i \neq j$, $\mathbb{J}_{ij}^{\mathcal{F}}$, $\mathbb{D}_{ij}^{\mathcal{F}}$ and $\mathbb{M}_{ij}^{\mathcal{F}}$ are identically zero while, for $i = j$, only $\mathbb{D}_{ii}^{\mathcal{F}}$ is identically zero whereas

$$\mathbb{J}_{ii}^{\mathcal{F}} = \begin{pmatrix} 0 & 0 & 0 \\ 0 & 0 & 0 \\ 0 & 0 & J^{\mathcal{F}} \end{pmatrix},\ \mathbb{M}_{ii}^{\mathcal{F}} = \begin{pmatrix} m_1^{\mathcal{F}} & 0 & 0 \\ 0 & m_2^{\mathcal{F}} & 0 \\ 0 & 0 & 0 \end{pmatrix},\ \text{for } i = j, \tag{4}$$

where $J^{\mathcal{F}}$, $m_1^{\mathcal{F}}$, $m_2^{\mathcal{F}}$ can be computed analytically, (see, for example, [6, Chapter 4]),

$$J^{\mathcal{F}} = \frac{1}{8}\rho\,\pi(a^2-b^2)^2\,,\ m_1^{\mathcal{F}} = \rho\,\pi b^2\,,\ m_2^{\mathcal{F}} = \rho\,\pi a^2\,. \tag{5}$$

The total kinetic energy of the solid-fluid system can then be written as

$$T = \frac{1}{2}\sum_i (\mathbf{\Omega}_i \cdot \mathbb{J}\,\mathbf{\Omega}_i + \mathbf{v}_i \cdot \mathbb{M}\,\mathbf{v}_i)\,, \tag{6}$$

where $\mathbb{J}$ and $\mathbb{M}$ refer to the total mass plus added mass 3×3 diagonal matrices: the first two diagonal entries of $\mathbb{J}$ are zero while the third is $J = J^{\mathcal{B}} + J^{\mathcal{F}}$; the first diagonal entry of $\mathbb{M}$ is $m_1 = m^{\mathcal{B}} + m_1^{\mathcal{F}}$, the second is $m_2 = m^{\mathcal{B}} + m_2^{\mathcal{F}}$ and the third is zero.

Let $\mathbf{p}_i$ denote the linear momentum of $\mathcal{B}_i$ expressed in inertial frame and $\mathbf{P}_i$ be that expressed in body frame. Also, let $\boldsymbol{\pi}_i$ denote the angular momentum of $\mathcal{B}_i$ taken about the origin of the inertial frame and $\mathbf{\Pi}_i$ be the angular momentum about the center of mass expressed in body frame. The following transformation relations hold

$$\boldsymbol{\pi}_i = \mathbf{Q}_i\mathbf{\Pi}_i + \mathbf{x}_i \times \mathbf{p}_i, \qquad \mathbf{p}_i = \mathbf{Q}_i\mathbf{P}_i\,, \tag{7}$$

where $\mathbf{P}_i$ and $\mathbf{\Pi}_i$ can be computed from the kinetic energy in Eqn. (6); namely, $\mathbf{P}_i = \dfrac{\partial T}{\partial \mathbf{v}_i} = \mathbb{M}\mathbf{v}_i$ and $\mathbf{\Pi}_i = \dfrac{\partial T}{\partial \mathbf{\Omega}_i} = \mathbb{J}\mathbf{\Omega}_i$. Assume that there are no external forces and moments acting on the body-fluid system, that is, one only has constraint forces at the joints and torques due to the torsional springs at the joints. Also, for concreteness, assume that the

[1] Recall that the links are neutrally buoyant, that is, the density of the body is equal to that of the fluid and that the body-fixed frames are placed at the respective mass centers.

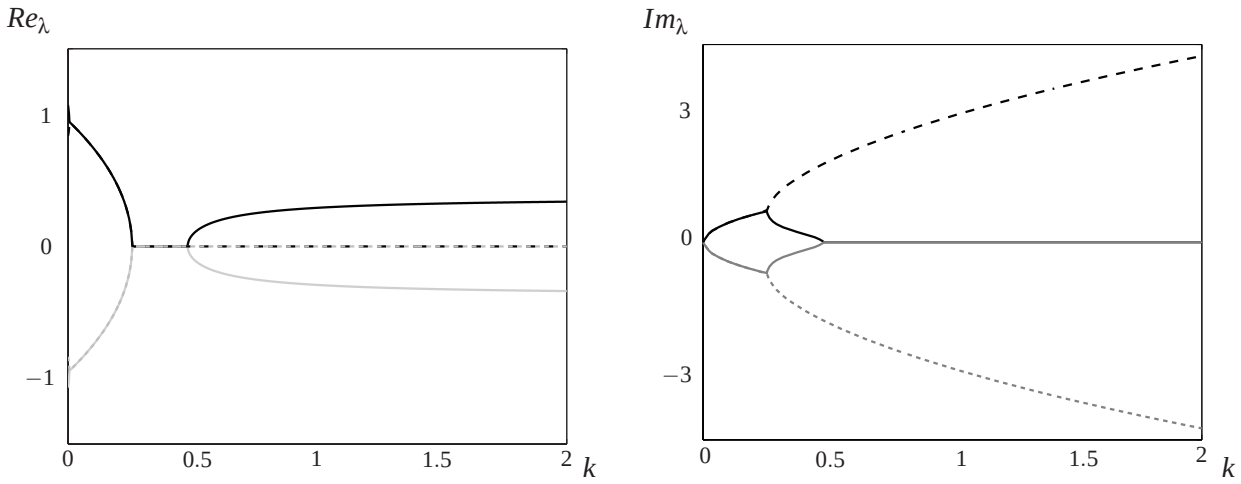

Figure 2. TWO-LINK MODEL: REAL AND IMAGINARY PARTS OF ALL NON ZERO EIGENVALUES OF THE LINEARIZED EQUATIONS OF MOTION FOR $b = 0.2$ WHILE VARYING k. THE REGION WITH ZERO REAL PART INDICATES A REGION OF LINEAR STABILITY.

articulated body consists of two links (ellipses) connected via one joint, that is, $i = 1, 2$. Note that the derivation of the equations of motion for the two-link body can be readily generalized to N links. One gets

$$\begin{aligned} \dot{\boldsymbol{\pi}}_1 &= (\mathbf{x}_1 + \mathbf{Q}_1\mathbf{r}_1) \times \mathbf{f}_c + \boldsymbol{\tau}, \qquad & \dot{\mathbf{p}}_1 &= \mathbf{f}_c, \\ \dot{\boldsymbol{\pi}}_2 &= (\mathbf{x}_2 - \mathbf{Q}_2\mathbf{r}_2) \times (-\mathbf{f}_c) - \boldsymbol{\tau}, \qquad & \dot{\mathbf{p}}_2 &= -\mathbf{f}_c, \end{aligned} \tag{8}$$

where $\mathbf{f}_c$ is the constraint force at the joint and $\boldsymbol{\tau} = k_1\theta_1\mathbf{e}_3$ (or simply $\boldsymbol{\tau} = k\theta\,\mathbf{e}_3$ for two links) is the internal torque applied at the joint by the torsional spring. If the constraint forces need not to be solved explicitly, the equations governing the linear momenta $\mathbf{p}_1$ and $\mathbf{p}_2$ may be combined into one equation governing the total linear momentum of the two-link body and the equations governing the angular momenta $\boldsymbol{\pi}_1$ and $\boldsymbol{\pi}_2$ may be expressed relative to the joint position (hence eliminating the torque due to the constraint force $\mathbf{f}_c$). Following these steps, then transforming the result into body frame, one gets the following set of equations governing the motion of the two-link body

$$\begin{aligned} \dot{\boldsymbol{\Pi}}_1^{joint} + (\mathbf{v}_1 + \boldsymbol{\Omega}_1 \times \mathbf{r}_1) \times \mathbf{P}_1 &= \boldsymbol{\tau}, \\ \dot{\boldsymbol{\Pi}}_2^{joint} + (\mathbf{v}_2 - \boldsymbol{\Omega}_2 \times \mathbf{r}_2) \times \mathbf{P}_2 &= -\boldsymbol{\tau}, \\ \dot{\mathbf{P}}_s + \boldsymbol{\Omega}_1 \times \mathbf{P}_s &= 0, \end{aligned} \tag{9}$$

where $\boldsymbol{\Pi}_1^{joint} = \boldsymbol{\Pi}_1 - \mathbf{r}_1 \times \mathbf{P}_1$ is expressed in the $\mathcal{B}_1$-frame and $\boldsymbol{\Pi}_2^{joint} = \boldsymbol{\Pi}_2 + \mathbf{r}_2 \times \mathbf{P}_2$ is expressed in the $\mathcal{B}_2$-frame, while $\mathbf{P}_s = \mathbf{P}_1 + \mathbf{R}_1\mathbf{P}_2$ is expressed in the $\mathcal{B}_1$-frame.

One could introduce the velocity of the joint $\mathbf{v} = \mathbf{v}_1 + \boldsymbol{\Omega}_1 \times \mathbf{r}_1 = \mathbf{R}_1(\mathbf{v}_2 - \boldsymbol{\Omega}_2 \times \mathbf{r}_2)$. Let $\mathbf{v} = v_x\mathbf{b}_1^1 + v_y\mathbf{b}_2^1$, that is, (v_x, v_y) are the components of the joint velocity as expressed in the $\mathcal{B}_1$-fixed frame. The components of the joint velocity can be expressed in the $\mathcal{B}_2$-frame using the transformation $\mathbf{R}_1^T$, which yields $(v_x\cos\theta + v_y\sin\theta, -v_x\sin\theta + v_y\cos\theta)$. To this end, one can readily verify that, in component form, one has

$$\begin{aligned} \boldsymbol{\Pi}_1^{joint} &= \left[(J + m_2a^2)\Omega_1 - m_2av_y\right]\mathbf{b}_3^1, \\ \boldsymbol{\Pi}_2^{joint} &= \left[(J + m_2a^2)\Omega_2 + m_2a(-v_x\sin\theta + v_y\cos\theta)\right]\mathbf{b}_3^2, \end{aligned} \tag{10}$$

and

$$\begin{aligned} \mathbf{P}_1 &= m_1v_x\mathbf{b}_1^1 + m_2(v_y - a\Omega_1)\mathbf{b}_2^1, \\ \mathbf{P}_2 &= m_1(v_x\cos\theta + v_y\sin\theta)\mathbf{b}_1^2 + \\ &\quad + m_2\left[-v_x\sin\theta + v_y\cos\theta + a\Omega_2\right]\mathbf{b}_2^2. \end{aligned} \tag{11}$$

Now, substitute Eqn. (10,11) into Eqn. (9) and use $\Omega_2 = \Omega_1 + \dot{\theta}$ together with the transformation $\mathbf{R}_1$ between the $\mathcal{B}_1$- and $\mathcal{B}_2$-frames to get, after some manipulations, that Eqn. (9) give rise to 5 first-order, nonlinear, differential equations expressed in terms of the variables v_x, v_y, Ω_1,

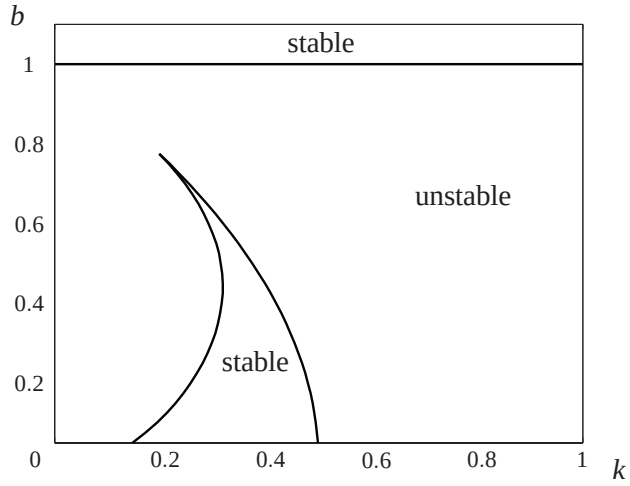

Figure 3. TWO-LINK MODEL: FULL PARAMETRIC ANALYSIS OF THE LINEAR STABILITY OF RELATIVE EQUILIBRIA q_e. ONE HAS TWO REGIONS OF LINEARLY STABILITY IN THE (b,k) PLANE.

θ and $\dot{\theta}$. These equations admit a family of relative equilibria of interest: the equilibria corresponding to the body-fluid system translating with an arbitrary constant velocity $v_x = U$ with no rotation and no internal shape deformation, i.e., with v_y, Ω_1, θ and $\dot{\theta}$ identically zero. For notational convenience, introduce $q = [v_x, v_y, \Omega_1, \theta, \dot{\theta}]^T$, the family of relative equilibria of interest can be expressed as

$$q_e = [U, 0, 0, 0, 0]^T . \tag{12}$$

We study the stability of these equilibria in section 3 but it is convenient beforehand to non-dimensionalize the equations by scaling all lengths with $\tilde{l} = \dfrac{l}{a}$, masses with $\tilde{m} = \dfrac{m}{\rho\pi a^2}$, and time with $\tilde{t} = \dfrac{t}{a/U}$. All terms can be readily non-dimensionalized accordingly, for example, one gets

$$\tilde{b} = \frac{b}{a}, \ \tilde{k} = \frac{k}{\rho\pi a^2 U^2}, \ \tilde{J} = \frac{J}{\rho\pi a^4}, \ \tilde{v}_x = \frac{v_x}{U}, \ \tilde{\Omega}_1 = \frac{\Omega_1}{U/a} . \tag{13}$$

We now drop the $\tilde{}$ notation with the understanding that all variables are non-dimensional.

3 STABILITY ANALYSIS

We analyze the stability of relative equilibria q_e in Eqn. (12) for body-fluid system using linearization method then verify the findings of our linear stability analysis using numerical simulations of the nonlinear equations. We begin by linearizing the equations of motion around the relative equilibria and examine the eigenvalues of the consequent linear system: if all eigenvalues have non-positive real parts, the corresponding relative equilibrium is said to be linearly or marginally stable (given that the system is conservative, i.e., no energy dissipation); if at least one eigenvalue has positive real part, the equilibrium is linearly unstable. Note that one can conclude nonlinear instability in Lyapunov's sense from linear instability. But linear stability does not necessarily indicate nonlinear stability, see, e.g., [8]. In this work, we do not analyze stability in the Lyapunov's sense rigorously, instead, we present numerical evidence (via numerical integration of the nonlinear equations) that the system might indeed be nonlinearly stable where it is linearly stable.

3.1 Two-link body

We perturb about the equilibrium in Eqn. (12) using $q = q_e + \delta q$, where $\delta q = [\delta v_x, \delta v_y, \delta\Omega_1, \delta\theta, \delta\dot{\theta}]^T$, then substitute q into Eqn. (9) and neglect higher order terms, the linearized equations of motion can be expressed in matrix form as

$$C\,\delta\dot{q} \;=\; D\,\delta q, \tag{14}$$

where

$$C = \begin{pmatrix} 1 & 0 & 0 & 0 & 0 \\ 0 & 2m_2 & 0 & 0 & 0 \\ 0 & 0 & 2(J+m_2a^2) & 0 & J+m_2a^2 \\ 0 & -m_2a & J+m_2a^2 & 0 & 0 \\ 0 & 0 & 0 & 1 & 0 \end{pmatrix},$$

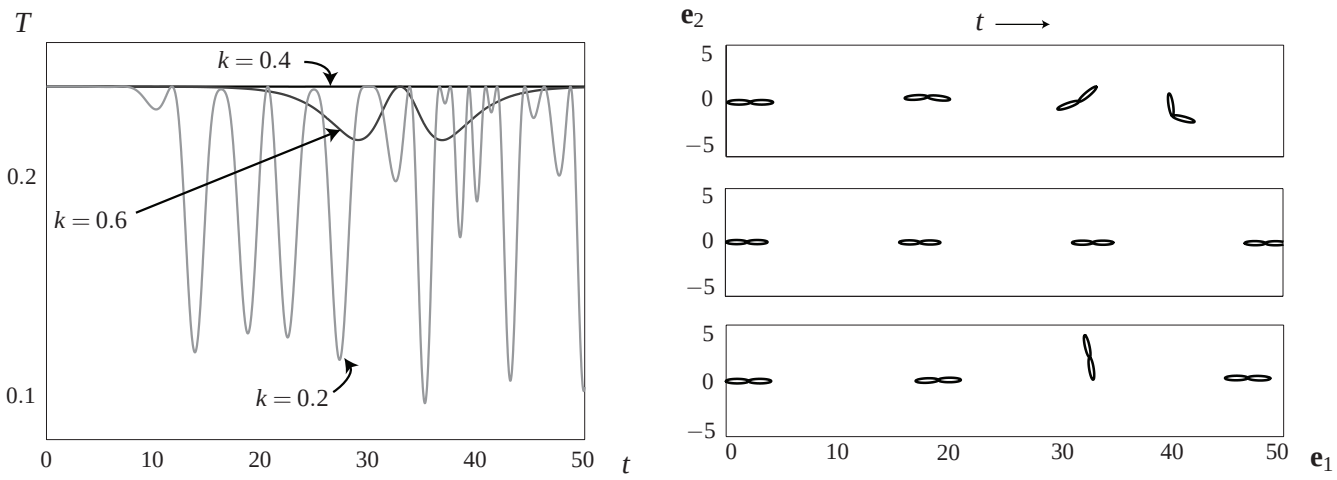

(a) Kinetic energy (b) Configurations at various times

Figure 4. TWO-LINK MODEL: (a) KINETIC ENERGY VERSUS TIME FOR THREE NUMERICAL SIMULATIONS WITH INITIAL CONDITIONS $q_0 = [1,0,0,0.001,0]^T$ AND TOTAL INTEGRATION TIME $t = 50$. THE THREE TRAJECTORIES CORRESPOND TO $b = 0.2$ WHILE $k = 0.2$, 0.4, AND 0.6, RESPECTIVELY. (b) SNAPSHOTS OF THE BODY CONFIGURATIONS AT $t = 0, 50/3, 100/3$, AND 50. (b)TOP CORRESPONDS TO $b = 0.2$, $k = 0.2$ (UNSTABLE); (b)MIDDLE CORRESPONDS TO $b = 0.2$, $k = 0.4$ (STABLE); and (b)BOTTOM CORRESPONDS TO $b = 0.2$, $k = 0.6$ (UNSTABLE).

and

$$D = \begin{pmatrix} 0 & 0 & 0 & 0 & 0 \\ 0 & 0 & -2m_1U & 0 & -\beta \\ 0 & 2\beta & 0 & -\beta U & 0 \\ 0 & \beta & m_2aU & k & 0 \\ 0 & 0 & 0 & 0 & 1 \end{pmatrix},$$

where $\beta = (m_1 - m_2)U$. The linear equations (14) may be equivalently written as

$$\delta\dot{q} \;=\; A\,\delta q, \qquad A \;=\; C^{-1}\,D. \tag{15}$$

Matrix A has 5 eigenvalues, denoted by λ_j, $j = 1,...,5$. Note that one of the eigenvalues (the one that corresponds to linearized equation in $\mathbf{b}_1^1$ direction) is always 0, which reflects a symmetry in the equations, namely, that q_e is a relative equilibrium for any U in $\mathbf{b}_1^1$ direction. Translations in $\mathbf{b}_1^1$ direction do not affect the equilibrium. The real and imaginary parts of the non-zero eigenvalues for a specific value of $b = 0.2$ are shown as a function of k in Fig. 2. One could readily identify a range of k values for which all eigenvalues have zero real part, which implied that the system is linearly stable for these parameter values. This is in contrast with stability result of a single submerged body, which is unstable for all $b < 1$, which means that, by allowing an internal shape change via θ, the two-link model shows that linear stability can be achieved for $b < 1$ given an appropriate value of k. Indeed, if k is small, which means the spring is weak, the model is similar to that of two independent ellipses (given the hydro-dynamically decoupled assumption), hence the system is unstable. If, on the other hand, k is too large, the spring is stiff and the model is similar to that of one single body (made of two ellipses), which is also unstable. For an intermediate range of k values which provide the appropriate bending resistance to perturbations, the system is stable. A full parametric analysis of the eigenvalues when varying both k and b suggests that, indeed, there is a region in the space (k,b) where two-link body is linearly stable region, see Fig. 3.

One could verify these stability results by direct numerical integration of the nonlinear equations of motion Eqn. (9) with initial condition slightly perturbed away from the relative equilibrium q_e. More specifically, we integrate the nonlinear equations from $t = 0$ to $t = 50$ with initial conditions $q(0) = [1,0,0,0.001,0]^T$, i.e. θ slightly perturbed from 0, for parameter values $b = 0.2$ and $k = 0.2, 0.4$

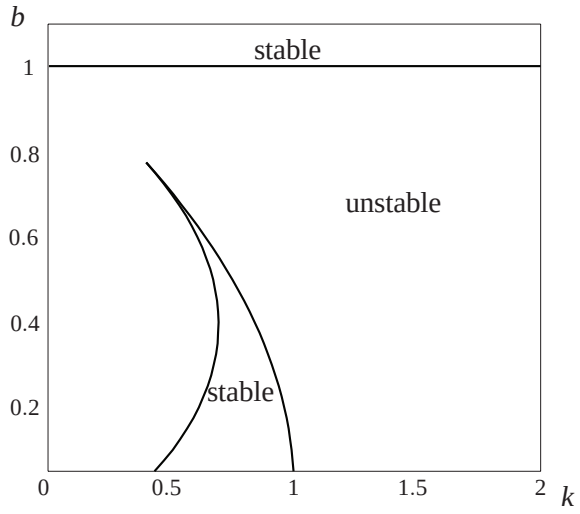

Figure 5. THREE-LINK MODEL: FULL PARAMETRIC ANALYSIS OF THE LINEAR STABILITY OF RELATIVE EQUILIBRIA q_e. ONE HAS TWO REGIONS OF LINEARLY STABILITY IN THE (b,k) PLANE.

and 0.6. The three distinct values of k correspond to values for which the systems is unstable ($k = 0.2$), stable ($k = 0.4$), and unstable ($k = 0.6$), as predicted by the linear stability results in Fig. 2. Figure 4(a) shows the kinetic energy of the system for these three cases. Clearly, for $k = 0.4$, the kinetic energy remains almost invariant reflecting the fact that the numerical solution stays close to the equilibrium which gives a numerical evidence that the system may also be nonlinearly stable. For $k = 0.2$ and $k = 0.6$, the kinetic energy varies dramatically which, given conservation of total energy of the system, means that the potential energy due to the torsional spring is also changing, that is, the shape variable θ deviates from its equilibrium value and that the system is unstable. In Fig. 4(b), we show snapshots of the body motion in the $(\mathbf{e}_1, \mathbf{e}_2)$ plane at $t = 0, 50/3, 100/3$, and 50 for all three cases. Clearly, the equilibrium is stable only when $k = 0.4$, while for $k = 0.6$ the body stumbles and for $k = 0.2$ the body stumbles and intersects itself.

3.2 Three-link body

Consider a three-link body where the links are made of identical ellipses (of major and minor axes a and b and uniform density ρ) and let θ_1 and θ_2 be the relative angles between $\mathcal{B}_1, \mathcal{B}_2$ and $\mathcal{B}_2, \mathcal{B}_3$, respectively. One could derive the equations of motion for the the three-link body in a similar way to the derivation presented in Section 2.2. To this end, one gets

$$\begin{aligned}
\dot{\mathbf{\Pi}}_1 + \mathbf{v}_1 \times \mathbf{P}_1 &= \mathbf{r}_1 \times (\dot{\mathbf{P}}_1 + \mathbf{\Omega}_1 \times \mathbf{P}_1) - \boldsymbol{\tau}_1, \\
\dot{\mathbf{\Pi}}_3 + \mathbf{v}_3 \times \mathbf{P}_3 &= -\mathbf{r}_3 \times (\dot{\mathbf{P}}_3 + \mathbf{\Omega}_3 \times \mathbf{P}_3) - \boldsymbol{\tau}_2, \\
\dot{\mathbf{\Pi}}_s + \mathbf{v}_2 \times \mathbf{P}_s &= 0, \\
\dot{\mathbf{P}}_s + \mathbf{\Omega}_2 \times \mathbf{P}_s &= 0,
\end{aligned} \tag{16}$$

where $\boldsymbol{\tau}_1 = k_1\theta_1\mathbf{b}_3^1$ and $\boldsymbol{\tau}_2 = k_2\theta_2\mathbf{b}_3^3$ are internal torque applied by the torsional springs, the total linear momentum of the system $\mathbf{P}_s = \mathbf{P}_2 + \mathbf{R}_1^{-1}\mathbf{P}_1 + \mathbf{R}_2\mathbf{P}_3$ is expressed in the $\mathcal{B}_2$-frame. The angular momenta $\mathbf{\Pi}_1, \mathbf{\Pi}_3$ in Eqn. (16) are taken about the center of mass of $\mathcal{B}_1$ and $\mathcal{B}_3$ respectively, while the total angular momentum of the system $\mathbf{\Pi}_s$ is taken about the center of mass of $\mathcal{B}_2$. The linear velocities $\mathbf{v}_i$ refer to the velocities of the mass center of $\mathcal{B}_i$ expressed in $\mathcal{B}_i$-frame. One could use the kinematic relations and the transformation matrices $\mathbf{R}_1$ and $\mathbf{R}_2$ to express all the variables in terms $\mathbf{v}_2$, $\mathbf{\Omega}_2$, θ_1, θ_2. One would then substitute these expressions into Eqn. (16) to get, after some manipulations, a system of 7 first-order, nonlinear ODEs in terms of the 7 variables $v_x, v_y, \Omega_2, \theta_1, \dot{\theta}_1, \theta_2$, and $\dot{\theta}_2$. Here, (v_x, v_y) are the components of $\mathbf{v}_2$ expressed in the $\mathcal{B}_2$ frame. Again, for notational convenience, introduce $q = [v_x, v_y, \Omega_2, \theta_1, \dot{\theta}_1, \theta_2, \dot{\theta}_2]^T$. The resulting set of equations admits a number of relative equilibria, the ones of importance here are the relative equilibria given by $q_e = [U, 0, 0, 0, 0, 0, 0]^T$. We analyze the linear stability of this family of equilibria as we did in Section 3.1 by perturbing a little bit away from the equilibirum $q = q_e + \delta q$. The linearized equations of motion have the same form as in Eqn. (14), but C and D are now given by

$$C = \begin{pmatrix}
1 & 0 & 0 & 0 & 0 & 0 & 0 \\
0 & 3m_2 & 0 & 0 & m_2a & 0 & -m_2a \\
0 & m_2a & J+2m_2a^2 & 0 & J+m_2a^2 & 0 & 0 \\
0 & -m_2a & J+2m_2a^2 & 0 & 0 & 0 & J+m_2a^2 \\
0 & 0 & J+4m_2a^2 & 0 & m_2a^2 & 0 & m_2a^2 \\
0 & 0 & 0 & 1 & 0 & 0 & 0 \\
0 & 0 & 0 & 0 & 0 & 1 & 0
\end{pmatrix}, \tag{17}$$

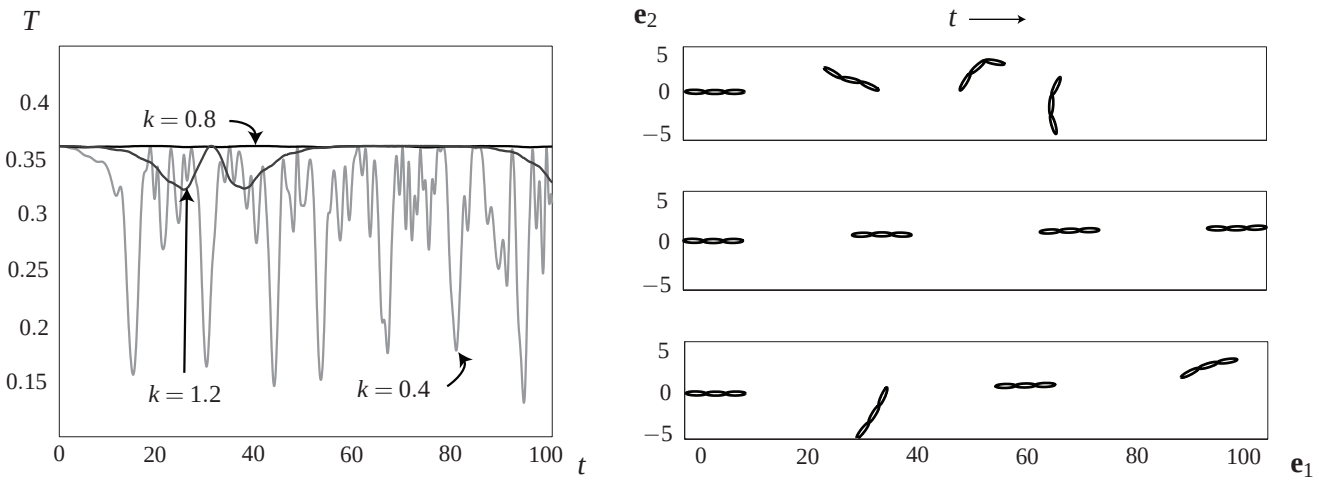

(a) Kinetic energy (b) Configurations at various times

Figure 6. THREE-LINK MODEL: (a) KINETIC ENERGY VERSUS TIME FOR THREE NUMERICAL SIMULATIONS WITH INITIAL CONDITIONS $q_0 = [1,0,0,0.01,0,-0.02,0]^T$ AND TOTAL INTEGRATION TIME $t = 100$. THE THREE TRAJECTORIES CORRESPOND TO $b = 0.2$ WHILE $k = 0.4$, 0.8, AND 1.2, RESPECTIVELY. (b) SNAPSHOTS OF THE BODY CONFIGURATIONS AT $t = 0, 100/3, 200/3$, AND 100. (b)TOP CORRESPONDS TO $b = 0.2$, $k = 0.4$ (UNSTABLE); (b)MIDDLE CORRESPONDS TO $b = 0.2$, $k = 0.8$ (STABLE); and (b)BOTTOM CORRESPONDS TO $b = 0.2$, $k = 1.2$ (UNSTABLE).

and

$$D = \begin{pmatrix} 0 & 0 & 0 & 0 & 0 & 0 & 0 \\ 0 & 0 & -3m_1U & 0 & -\beta & 0 & -\beta \\ 0 & \beta & \beta - m_2aU & -k_1 - \beta U & 0 & 0 & 0 \\ 0 & \beta & -\beta + m_2aU & 0 & 0 & -k_2 - \beta U & 0 \\ 0 & \beta & 0 & k_1 & -a\beta & k_2 & a\beta \\ 0 & 0 & 0 & 0 & 1 & 0 & 0 \\ 0 & 0 & 0 & 0 & 0 & 0 & 1 \end{pmatrix}. \tag{18}$$

Rewrite the linearized equation in the same form as Eqn. (15), matrix A has 7 eigenvalues, one of which is identically zero reflecting the symmetry due to translations in the $\mathbf{b}_1^2$ direction. Consider a special case when $k_1 = k_2 = k$. A full parametric analysis of the eigenvalues when varying both b and k is shown in Fig. 5. Note that, the stable region for $b < 1$ in three-link case has similar shape in comparison to the two-link case. However, for each b, the values of k, such that q_e is linearly stable, are generally larger than the corresponding two-link case. The area of stable region for three-link case is also bigger than two-link case. We integrate the nonlinear equations numerically for the initial conditions $q_0 = [1,0,0,0.01,0,-0.02,0]^T$ and for three sets of parameter values: $b = 0.2$ and $k = 0.4, 0.8,$ and 1.2. The kinetic energy associated with the obtained time solutions are shown in Fig. 6(a) which shows that, indeed, for $k = 0.8$, the system remains close to the equilibrium for all time from $t = 0$ to $t = 100$ whereas for $k = 0.4$ and $k = 1.2$ the system is unstable. The configuration of the system at 4 distinct time instants is shown in Fig. 6(b) for all three cases. One could analyze the behavior of the stability region in the (b,k) plane as the number of links N increases and eventually as $N \to \infty$, that is, for a fully deformable body (sustaining only bending deformations). Such analysis will be pursued in future works.

4 Summary

The equations of motion for a submerged deformable body are derived and the stability of an associated family of relative equilibria is studied. In comparison to the rigid body model in which these equilibria are unstable, one gets that by, introducing internal deformation variables, these equilibria can be stabilized for a range of parameter values. A summary of the stability results is shown in Tab. 1.

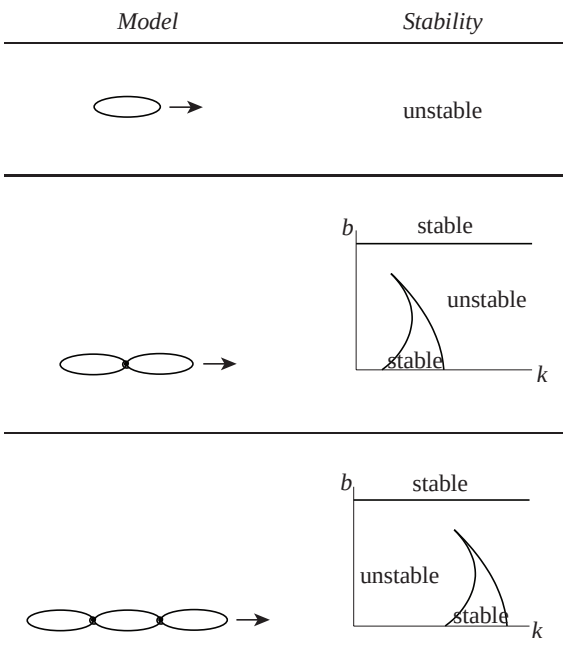

Table 1. SUMMARY OF STABILITY

ACKNOWLEDGMENT

The authors would like to thank Prof. Paul Newton for many useful discussions.

REFERENCES

[1] Kanso, E., Marsden, J.E., Rowley, C.W. and Melli-Huber, J. [2005], Locomotion of articulated bodies in a perfect fluid, *Journal of Nonlinear Science*, **15(**255–289).

[2] Lamb, S.H. [1932], *Hydrodynamics*, Cambridge University Press.

[3] Leonard, N.E. [1997], Stability of a bottom-heavy underwater vehicle, *Automatica*, **33(**331–346).

[4] Argentina, M. and Mahadevan, L. [2005], Fluid-flow-induced flutter of a flag, *PNAS*, **102**(1829-1834).

[5] Michelin, S., Smith, S.G.L., and Glover, B.J. [2008], Vortex shedding model of a flapping flag, *J. Fluid Mech.*, **617**(1–10).

[6] Newman, J.N. [1977], *Marine Hydrodynamics*, MIT press, Cambridge, Ma.

[7] Childress, S. [1981], *Mechanics of swimming and flying*, Cambridge University Press, NY.

[8] Marsden, J.E. [1992], *Lectures on Mechanics*, volume 174 of *London Math. Soc. Lecture Note Ser.* **174**, Cambridge University Press.